J Solid State Electrochem (2007) 11:1245–1252
DOI 10.1007/s10008-007-0279-3

ORIGINAL PAPER

EIS characterization of the evolution of calcium carbonate scaling in cooling systems in presence of inhibitors

J. Marín-Cruz · R. Cabrera-Sierra · M. A. Pech-Canul · I. González

Received: 9 October 2006 / Revised: 28 November 2006 / Accepted: 13 January 2007 / Published online: 15 February 2007

Abstract Electrochemical impedance spectroscopy (EIS) was used to assess the relative effects of scaling and corrosion for steel electrodes in cooling water media and to obtain information on corrosion inhibition and scale inhibition properties of 1-hydroxyethylidene-1,1-diphosphonic acid (HEDP) and hydroxyphosphonoacetic acid (HPA). Steel electrodes were preliminary scaled with $CaCO_3$ in simulated cooling water and then immersed in the characterization solution. Analysis of the impedance spectra with a simple model allowed following of the time evolution of physical parameters corresponding to the calcium carbonate islands and to the corrosion products accumulated in areas not covered by the scale. In uninhibited solutions, the main effect was the progressive deposit of corrosion products with no additional scaling and little restructuring of the initial carbonate islands. When the solution contained HEDP alone, part of the initial scale was detached from the surface, but the presence of HPA or the mixture HPA+HEDP only induced structural modifications of the initial scale. Moreover, the impedance analysis also showed that HPA exhibited better corrosion inhibition properties than HEDP.

Keywords Electrochemical impedance spectroscopy · Scaling · Corrosion · Carbon steel · Cooling waters · HEDP · HPA

J. Marín-Cruz (✉)
Coordinación de Ingeniería Molecular, Área de Materiales y Corrosión, Instituto Mexicano del Petróleo,
Eje Central Lázaro Cárdenas No. 152,
07730 Mexico, D.F., Mexico
e-mail: jmarin@imp.mx

R. Cabrera-Sierra
Academia de Química Analítica, Escuela Superior de Ingeniería Química e Industrias Extractivas (ESIQIE-IPN),
Edificio Z5. A.P:75-874,
07738 Mexico, D.F., Mexico

M. A. Pech-Canul
Departamento de Física Aplicada, Centro de Investigación y de Estudios Avanzados del IPN,
A.P. 73 Cordemex,
97310 Merida, Yucatan, Mexico
e-mail: max@mda.cinvestav.mx

I. González
Departamento de Química, Universidad Autónoma Metropolitana,
Apdo. Postal 55-534, 09340 Mexico, D.F., Mexico
e-mail: igm@xanum.uam.mx

Introduction

Due to time and operation conditions, industrial cooling systems show the formation of corrosion, scale, and bacteriological products on the metallic surfaces. Despite of the application and the development of inhibitors and biocides, the complex interrelations between these products make the control of corrosion and scaling phenomena very difficult.

One of the main problems in cooling systems is generated by scaling. This phenomenon is mainly associated with the loss of capacity for thermal exchange. Because cooling systems are multicomponent, i.e., characterized by the presence of a great variety of ions, the likelihood of many reactions increases the complexity of the scaling process. In general, scaling problems are mainly associated with the precipitation of phosphate salts, silica, and calcium carbonate, this latter being the most common type of scale deposit in cooling systems [1–6].

On the other hand, the anodic dissolution of steel produces Fe(II) ions, which, due to interaction with ions present in the water such as hydroxides, carbonates, phosphates, and sulfates, can precipitate forming a variety of scale and/or corrosion products.

Electrochemical techniques have been successfully applied in the study of corrosion [7–10] and scaling phenomena in different systems [11–21]. However, in real operating conditions, both phenomena occur simultaneously. Thus, studies focused on understanding the relations between corrosion and scaling processes are of great scientific and technological interest.

In this work, carbon steel electrodes were electrochemically scaled with calcium carbonate from simulated cooling water and immediately transferred to low-calcium cooling water (characterization solution), where they were allowed to corrode freely under open circuit conditions. Thus, upon immersion in the characterization solution, the surface morphology became gradually modified by the possible evolution of the scale layer itself and by the formation of corrosion products. The first objective was to study such evolution of the interface within the first hours of immersion using EIS. The second objective was to investigate how such complex layer is modified due to the separate or simultaneous presence in the solution of two chemicals often used in cooling water treatment [hydroxyphosphonoacetic acid (HPA) and 1-hydroxyethylidene-1,1-diphosphonic acid (HEDP)].

Experimental

The study was carried out using a standard three-electrode cell. The reference was a saturated calomel electrode (SCE), and the counter electrode was a graphite bar. The working electrode was a 1018 carbon steel disc with surface area of 0.5 cm^2; its surface was prepared by mechanical polishing with silicon carbide paper no. 600 and then cleaned by ultrasonic washing in acetone for 5 min.

The simulated cooling water used for the electrochemical scaling of the steel electrodes (hereafter known as AS3C) had the following composition: 9.0×10^{-3} M $CaCO_3$ [360 mg/l Ca(II)]; 1.5×10^{-3} M $MgCl_2.6H_2O$ [150 mg/l Mg (II)]; 8.3×10^{-4} M SiO_2 [50 mg/l SiO_2]; 4.0×10^{-3} M Na_2SO_4 [200 mg/l SO_4(−II)]; 2.6×10^{-3} M NaCl [200 mg/l Cl(−I)]; 1.1×10^{-3} M NaH_2PO_4 [10 mg/l PO_4(−III)], and 3.6×10^{-6} M $FeSO_4.7H_2O$ [0.1 mg/l Fe(II)]. The characterization solution (hereafter known as AS) had a similar composition, except that the calcium concentration was one third of that used in the AS3C solution. Both solutions (AS3C and AS) were prepared using a commercial soluble silicate (sodium silicate) containing 26% weight of SiO_2 and 7.5% weight of Na_2O; in this way, to obtain a concentration of 50 mg/l of SiO_2, 192.3 mg/l of soluble silicate was used. The AS composition represents the average concentration of salts present in the waters used in Mexican cooling towers. The pH of both solutions was adjusted to 7.8. For inhibited solutions, a typical dosage of 3 mg/l was used for each inhibitor. The mixture contained 3 mg/l of HEDP and 3 mg/l of HPA.

In both stages of the experiment (scaling+immersion in the characterization solution), the solutions were maintained at 40 °C, and the working electrode was rotated at 2,000 rpm. Electrochemical impedance measurements were carried out with an Autolab PGSTAT30 with FRA2 module in the frequency range between 50 KHz and 10 mHz.

Scale induction

Several ways of scaling metal surfaces with calcium carbonate have been informed in the literature [22–26]; based on a methodology previously developed by our research group to selectively induce calcium carbonate scales with different allotropic forms [19, 20], the rotating carbon steel electrodes were scaled by applying a potential of −1.1 V vs SCE for 10 min in the AS3C solution. According to the previous study [20], such potential allowed the deposition of calcium carbonate predominantly in the form of aragonite.

Scaled surface evolution as a function of time

In an earlier study [27], we observed that the impedance response of a (non-scaled) carbon steel electrode immersed in the AS solution is not significantly modified after a 5-h immersion; a similar behavior was observed in this work for the scaled electrodes.

The surface of scaled electrodes was examined after 10 min and after 5 h of immersion in the AS solution using a Philips XL30 ESEM for environmental scanning electron microscopy (ESEM). Figure 1 shows evidence of the changes in surface morphology due to immersion in such medium.

Model

Figure 1 suggests that in the uninhibited low-calcium solution the initial deposit pattern of aragonite clusters remains almost unaltered. The scale may have suffered slight structural changes during immersion in the AS solution; however, it appears that the further deposition or further growth of calcium carbonate crystals was negligible. The SEM micrographs in Fig. 1 show evidence that evolution in the morphology occurred mainly in the areas surrounding the aragonite clusters. The non-scaled parts of the surface became covered by a layer, which consists most likely of corrosion products. The formation of a uniform layer of $Mg(OH)_2$ is unlikely due to lack of sufficiently alkaline conditions. Thus, as a first approximation, the interface can be modeled (see

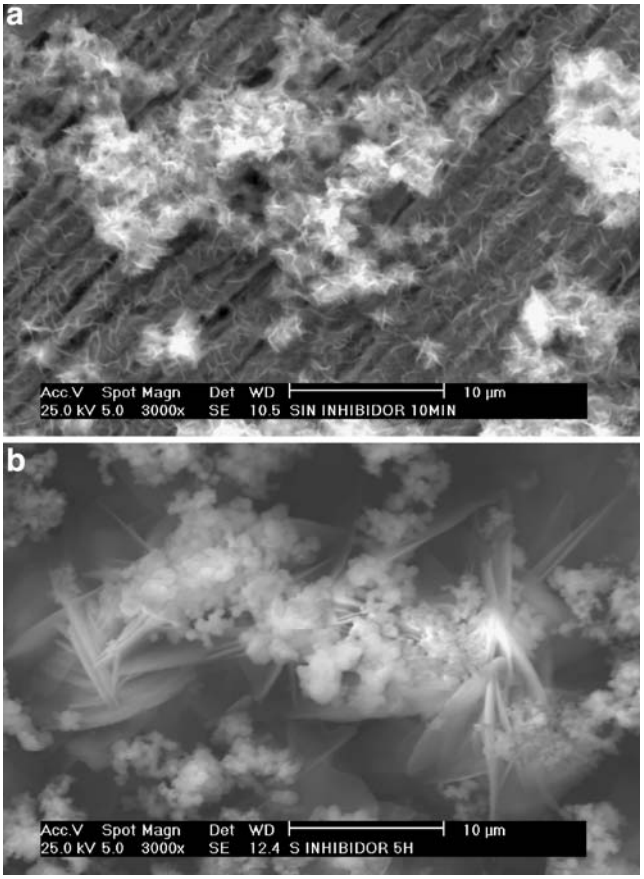

Fig. 1 SEM micrographs of scaled electrode after **a** 10 min and **b** 5 h immersion in the characterization solution AS

schematic representation in Fig. 2) assuming that one part of the metallic surface (S_2) is covered by calcium carbonate islands and the remaining part (S_1) by corrosion products. Taking into account that the impedance response of each of these parts is Z_2 and Z_1, respectively, and that the scale coverage is given by $\theta = S_2/(S_1 + S_2)$, the overall impedance response Z would be given by

$$(Z - R_s)^{-1} = \theta Z_2^{-1} + (1-\theta)Z_1^{-1} \quad (1)$$

where R_s is the solution resistance.

Our previous research [21] showed that, for electrodes that were electrochemically scaled in the AS3C solution, the convective flow effect on the impedance response is negligible. Thus, the impedance of the blocked area S_2 is, according to Jaouhari et al. [17],

$$Z_2 = \left[R_f(1 + j\omega C_f R_f)^{-1}\right] + (\rho Z_0)^{1/2} \operatorname{cotanh}\left(L(\rho/Z_0)^{1/2}\right) \quad (2)$$

where:

$$Z_0 = \left[R_t(1 + j\omega C_d R_t)^{-1}\right]. \quad (3)$$

The first term in the right side of Eq. 2 corresponds to the impedance of the scale layer itself with R_f and C_f being the resistance of the electrolyte inside the pores and dielectric capacitance of the scale, respectively. The second term involves charge transfer R_t of oxygen, distributed due to ohmic drop in the cavities under the scaling blocks. C_d is the double layer capacitance, L the length of the interstices between the $CaCO_3$ crystal and the metallic surface, and ρ the resistance per unit length of the cavity given by

$$\rho = L/\gamma\pi r^2 \quad (4)$$

where r is the radius of the cavities and γ the conductivity of the solution inside.

For the corroded surface, Z_1 consists of C_d in parallel with the faradaic impedance of oxygen reduction reaction, represented by the charge transfer resistance plus the diffusional impedance (involving the diffusion resistance R_d and the time constant for diffusion through the corrosion products τ_p)

$$Z_1^{-1} = j\omega C_d + \left[\boldsymbol{R_t} + \boldsymbol{R_d}\ \tanh\left(j\omega\tau_p\right)^{1/2} \Big/ \left(j\omega\tau_p\right)^{1/2}\right]^{-1}. \quad (5)$$

From Eqs. 1, 2, and 5 and considering the blocking parameter $\sigma = S_2/S_1$, the total transfer function for the

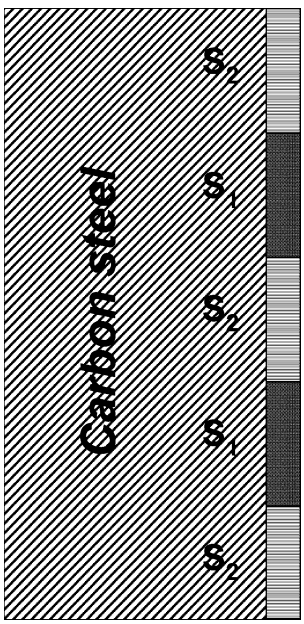

Fig. 2 Schematic representation of electrode covered by scale/corrosion layer; S_1, area covered by corrosion products and S_2, area covered by $CaCO_3$ islands

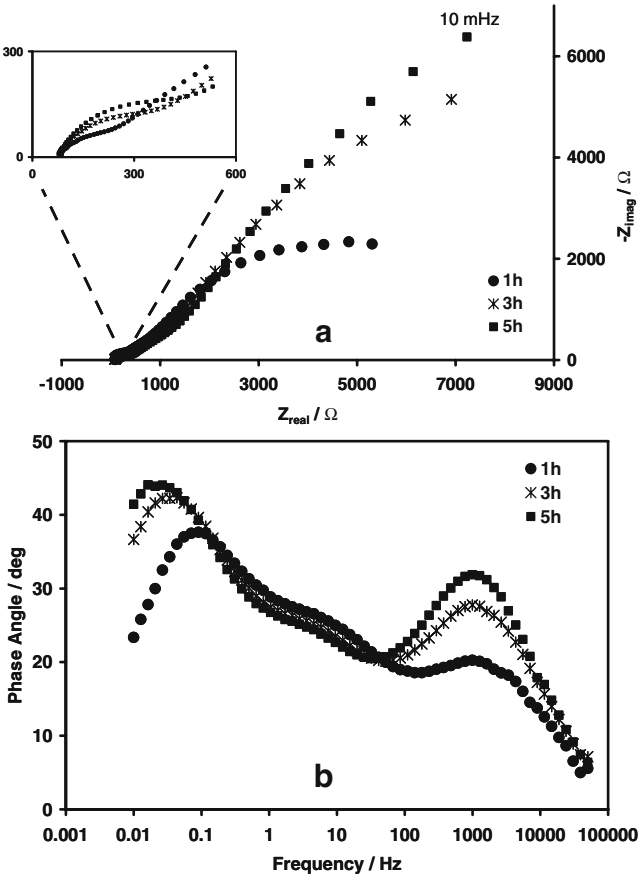

Fig. 3 Impedance spectra obtained for the scaled electrode after three immersion times in the characterization solution AS, represented in the **a** Nyquist and **b** phase–Bode plots

electrode (partly covered by scale and partly covered by corrosion products) is

$$(Z - R_s)^{-1} = (1+\sigma)\left[\boldsymbol{R_t} + \boldsymbol{R_d}\ \tanh\left(j\omega\tau_p\right)^{1/2} \Big/ \left(j\omega\tau_p\right)^{1/2}\right]^{-1} + \sigma[Z_s(1+\sigma)]^{-1} + j\omega C_d(1+\sigma)^{-1}. \quad (6)$$

Results and discussion

EIS characterization of scaled surface evolution

In Fig. 3, typical impedance spectra for scaled electrodes immersed in the characterization solution are presented. Measurements were made consecutively for three immersion times (1, 3, and 5 h). The Nyquist diagrams look highly depressed and exhibit three arcs in the frequency range

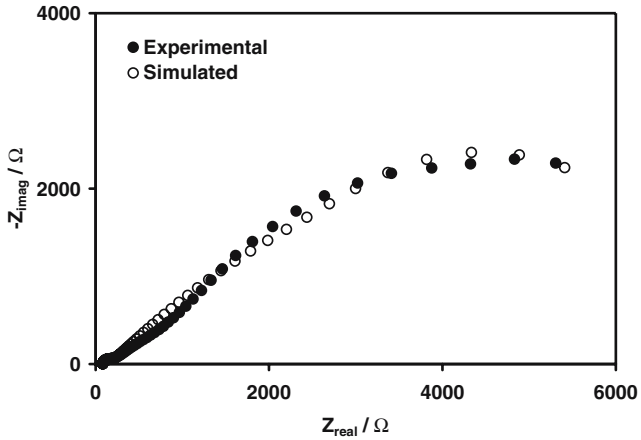

Fig. 4 Comparison between experimental and simulated spectra using as an example the data for 1 h immersion in AS solution without inhibitors. Simulation was made with Eq. 6 using parameters in Table 1

investigated. As suggested above from observation of SEM micrographs, the layer covering the metallic surface consisted initially of $CaCO_3$ islands, and upon immersion in the AS solution, it evolved to a complex layer containing scale and corrosion products. As a result of this evolution, the high frequency (HF) and low frequency (LF) arcs of the complex impedance diagrams exhibited increasing size with immersion time, whereas the medium frequency (MF) arc remained nearly unchanged. The shape of the bode plots suggests that the HF arc does not correspond to a single time constant (e.g., due to the dielectric capacitance of the scale in parallel with the resistance of electrolyte inside the pores); this effect is most likely due to modifications in scale properties by the presence of corrosion products. With regard to the LF arc, its low characteristic frequency suggests that it corresponds to a process of oxygen diffusion through the scale-corrosion layer.

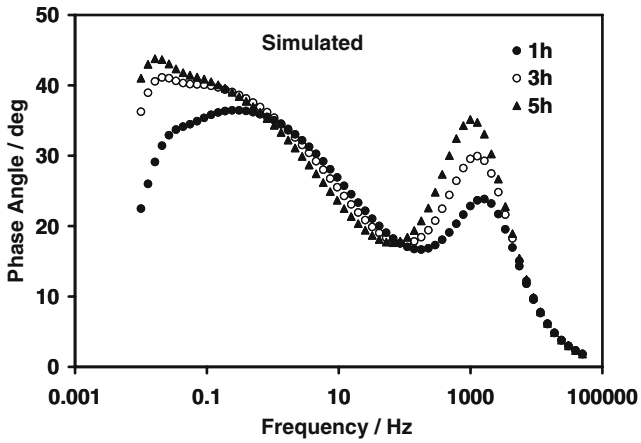

Fig. 5 Simulated impedance spectra in the phase–Bode plot corresponding to the experimental spectra presented in Fig. 3. Simulations were made with Eq. 6 using parameters reported in Table 1

Table 1 Time evolution of parameters (obtained by the best fit in the simulation of EIS spectra using Eq. 6) associated to corrosion and scale processes due to immersion of the scaled electrode in uninhibited AS solution

Immersion time (h)	σ	R_f (Ω)	C_f (F)	ρ	C_d (F)	$L/10^{-4}$ (cm)	R_t (Ω)	R_d (Ω)	τ_p (s)
1	8.15	1,450	1×10^{-8}	3,900,961	1.05×10^{-5}	12	10.7	1,530	48
3	8.15	1,450	1×10^{-8}	3,900,961	1.05×10^{-5}	3.17	16.1	1,840	62
5	8.15	1,450	1×10^{-8}	3,900,961	1.05×10^{-5}	0.995	22.4	1,977	67

Furthermore, as shown by the phase Bode plot in Fig. 3b, the characteristic frequency of such LF arc is shifted towards lower frequencies with immersion time, giving indication of an increment in the diffusion time constant.

A more detailed analysis of the impedance spectra was carried out by fitting experimental data to Eq. 6 using a nonlinear minimum square fitting procedure in Mathematica Software. Figure 4 shows a comparison between the experimental impedance spectrum corresponding to 1-h immersion and a spectrum simulated using Eq. 6. In Fig. 5, the simulated spectra for the three immersion times are presented as phase Bode plots. Table 1 reports the values obtained for the different parameters from the best fit of the experimental spectra. From Fig. 4 and comparison of Figs. 3b and 5, it can be observed that, except for a slight discrepancy in the MF range, the model does mimic reasonably well all the features of the experimental impedance diagram. Further evidence that the model represents a good approximation is the fact that the parameters used in the simulations (reported in Table 1) are within the limits of physical sense and show trends that are consistent with the evolution of the layer's morphological features discussed above.

The constant value of σ suggests that the scale coverage did not vary while the electrode was immersed in the AS solution (i.e., additional deposition of $CaCO_3$ in this solution was negligible). As the resistance and capacitance associated with the scale (R_f and C_f) remained constant, there is also an indication that there was no evolution in the thickness or the porosity of the calcium carbonate scale covering the area S_2. However, the length of the interstices L decreased with immersion time; considering that ρ did not suffer variations (Table 1) and assuming that γ was approximately constant, it turns out (from these results and Eq. 4) that the mean radius of the cavities also decreased. Such an effect is probably due to the formation of corrosion products within the cavities.

Concerning the area covered by corrosion products (S_1), the increasing values of diffusion resistance (R_d) and time constant (τ_p) reported in Table 1 suggest that the oxygen diffusion rate through these products decreased with immersion time. Such an effect, along with the observed increment in the R_t values, provides evidence of oxygen reduction inhibition.

Inhibitors effect

In Fig. 6, typical impedance spectra obtained after 5-h immersion in inhibited AS solutions are presented. For comparison, the impedance spectrum for the blank (corresponding to 5-h immersion) is also included. Figure 6a shows that the size of the LF arc followed the sequence: blank>mixture>HPA>HEDP, being the largest for the blank. Furthermore, from the Bode phase angle plots in Fig. 6b, two main changes in the frequency response due to the presence of inhibitors are evident: (1) the LF and MF features intermingled, and (2) the HF feature manifested shrinkage. This later effect was more important in the

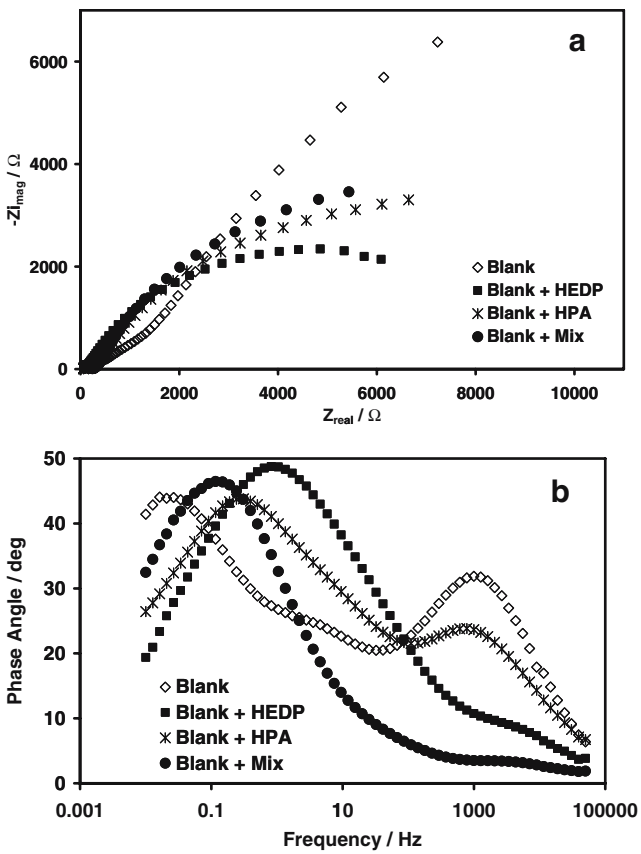

Fig. 6 Impedance spectra obtained for the scaled electrode after 5 h immersion time in AS solutions containing HEDP, HPA, or a mixture HEDP+HPA. For comparison, the data corresponding to uninhibited AS solutions is also included. **a** Nyquist and **b** phase–Bode plots

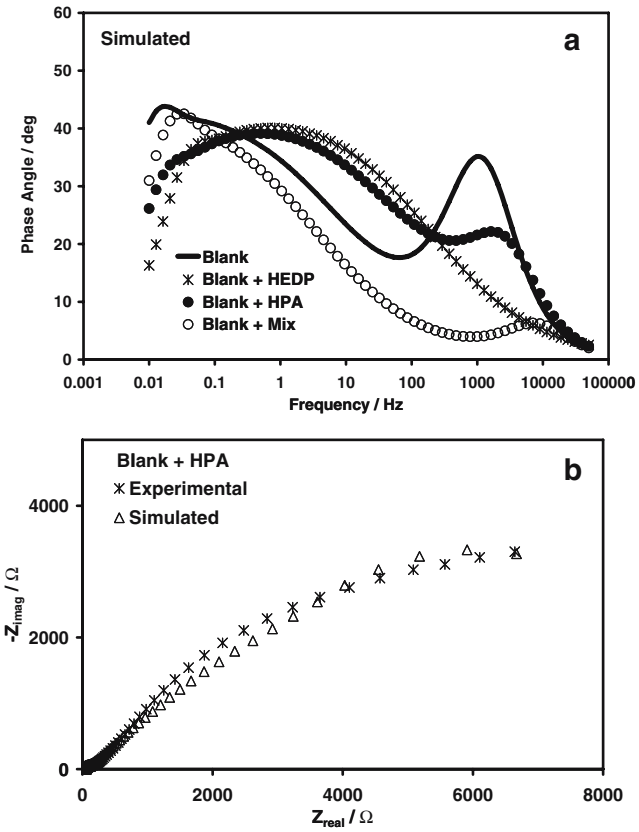

Fig. 7 **a** Simulated impedance spectra in the phase–Bode plot corresponding to the experimental spectra presented in Fig. 6. Simulations were made with Eq. 6 using parameters reported in Table 2. **b** Comparison between experimental and simulated spectra in the Nyquist plot using as an example the data for scaled electrode in AS solution+HPA

presence of HEDP than in the presence of HPA. Evidently, the electrochemical impedance technique is very sensitive to morphological changes induced by the presence of these inhibitors. It is proper to mention that a tangible change in the impedance responses could result from the inhibitor effect at the beginning of the immersion time. In fact, the main modifications by the inhibitors, at low immersion times, are observed at HFs in the EIS spectra, increasing the phase angle value reaching the maxima values at 5 h of immersion. For clarity, only the spectra obtained at this time (5 h) were considered hereafter. To get an insight into the physical meaning of these modifications in the impedance response, an attempt to analyze the spectra in Fig. 6, with the transfer function given by Eq. 6, was made. The experimental spectra were fitted through the Eq. 6 using a nonlinear minimum square fitting procedure in Mathematica Software. The corresponding simulated spectra are presented as Bode phase plots in Fig. 7a (parameters used in the simulation are reported in Table 2). As an example for the case of HPA, Fig. 7b shows a comparison between experimental and simulated spectra in the Nyquist representation. Comparison of Figs. 6b and 7a shows that the model does mimic reasonably well the LF and HF ends of the impedance spectra, but not so well as the response in the MF range. Nevertheless, Fig. 7b suggests that the discrepancy between the model and experiment in that frequency range is minor. From this observation, we conclude that the model is still applicable even when the scaled electrodes were immersed in inhibited solutions.

The above discussion of surface evolution in the absence of inhibitors showed that the scale/corrosion layer exhibited cathodic inhibition properties. A comparison of the R_t and τ_p values in Table 2 seems to suggest that such properties for the layer developed in the blank are better than those for the layers developed in the presence of inhibitors. This is because, in the presence of inhibitors, the $CaCO_3$ islands are either partially removed (when σ decreases) or undergo structural modifications (e.g., become more porous as R_f decreases); in the blank, the initial scale remains almost intact. It is actually a consequence of the methodology used in this work: The steel electrode was preliminary scaled by electrodeposition in a concentrated calcium solution and then transferred to a characterization solution without and with additions of inhibitors. Although it is not completely representative of a complex real situation, in which scale and corrosion products develop simultaneously at open circuit conditions, and despite of the peculiarity for R_t between blank and inhibited solutions, we found that this methodology was very useful to discriminate the relative contribution of each inhibitor added alone or in a mixture (see below).

It is well known that HEDP is one of the most effective inhibitors for calcium carbonate, and results of the impedance analysis are in agreement with such behavior. The value of σ decreased from 8.15 to 1 (see Table 2), and

Table 2 Parameters (obtained by the best fit in the simulation of EIS spectra using Eq. 6) associated to corrosion and scale processes corresponding to 5 h immersion of the scaled electrode in uninhibited (AS) and inhibited solutions

	σ	R_f (Ω)	C_f (F)	ρ	C_d (F)	$L/10^{-4}$ (cm)	R_t (Ω)	R_d (Ω)	τ_p (s)
AS	8.15	1,450	1×10^{-8}	3.9×10^{6}	1.05×10^{-5}	0.995	22.4	1,977	67
AS+HEDP	1	200	1×10^{-8}	6.45×10^{7}	1×10^{-7}	2.9	1	5,780	25
AS+HPA	10	620	1×10^{-8}	1.6×10^{7}	1.4×10^{-5}	3.5	5	1,720	59
AS+mix	10	830	1×10^{-8}	6.45×10^{7}	4×10^{-6}	0.12	5	730	35

the HF arc nearly disappeared, thus giving indication of scale removal in the presence of HEDP. Moreover, the remaining $CaCO_3$ islands exhibited a lower resistance R_f (indicating that are more porous) and had larger length of cavities (L) than the scale covering the electrode area S_2 in the blank solution. As a result of scale removal, the charge transfer resistance (R_t) decreased and the corrosion rate increased; in addition, the rate of oxygen diffusion through the corrosion products was higher in this case (τ_p decreased from 67 to 25). These latter two observations are consistent with the shrinkage of the LF arc observed in Fig. 7a. Although it is often acknowledged that HEDP may also act as a corrosion inhibitor [9, 28, 29], it appears that, for the particular experimental conditions used in this work, its main effect was to remove calcium carbonate scale.

HPA is also known to exhibit dual properties; however, there seems to be the general agreement that it is a relatively ineffective scale inhibitor and that it mostly behaves like a corrosion inhibitor [4, 28, 29]. Comparing the parameter values in Table 2 for the blank and blank+HPA, it is observed that the blocking parameter did not decrease (in fact, it increased slightly from 8.15 to 10). Thus, scale coverage remained almost unchanged in the presence of HPA. However, as evidenced by the slight shrinkage of the HF feature (Fig. 6b) and by changes in R_f, ρ, and L, the presence of HPA induced structural modifications in the $CaCO_3$ scale. The film resistance decreased and also did the diameter of cavities under carbonate crystals (as calculated from Eq. 4, using the values of ρ and L reported in Table 2). With respect to its effect on the corrosion process, Neagle [4] suggested that HPA forms complexes with Ca^{2+} ions in the solution and then provides cathodic inhibition by forming a tenacious film at cathodic sites. Comparing the charge transfer resistance values in Table 2, it is observed that the one corresponding to the solution with HPA is higher than that corresponding to the solution with HEDP, thus confirming that HPA has better corrosion inhibition properties than HEDP.

In the presence of a mixture of both compounds, scale coverage remained almost unchanged with respect to that in the blank (σ did not decrease), but similarly to the observed when only HPA was added to the characterization solution, a structural modification of the $CaCO_3$ islands took place (R_f, L, and r decreased while ρ increased). A comparison of the parameter values for the mixture with respect to those for HEDP and HPA shows that the value of R_f followed the sequence: mixture>HPA>HEDP, suggesting that for the mixture, the scale is less porous. Furthermore, both the L and r values (calculated from Eq. 4 and values of ρ and L in Table 2) decrease in the mixture, indicating a reduction in the size of cavities under aragonite crystals. Despite of these morphological changes due to the simultaneous presence of both compounds, the corrosion inhibition properties did not improve with respect to those for HPA alone (the R_t values were the same for HPA and for the mixture).

Conclusions

EIS was used to assess the relative effects of scaling and corrosion for steel electrodes in cooling waters and to obtain information on corrosion inhibition and scale inhibition properties of two chemicals, which act on calcium carbonate scales. The experimental protocol involved two stages: electrodeposition of a $CaCO_3$ layer on steel electrodes in simulated cooling water and then immersion of the scaled electrodes in the characterization solution. Analysis of the impedance spectra with a simple model allowed following of the time evolution of physical parameters corresponding to the calcium carbonate islands and to the corrosion products accumulated in areas not covered by the scale. In uninhibited solutions, the main effect was the progressive deposit of corrosion products with no additional scaling and little restructuring of the initial carbonate islands. When the solution contained HEDP alone, part of the initial scale was detached from the surface, but the presence of HPA or the mixture HPA+HEDP only induced structural modifications of the initial scale. Moreover, the impedance analysis also showed that HPA exhibited better corrosion inhibition properties than HEDP.

References

1. Dubin L (1980) National Association of Corrosion Engineers Annual Meeting 80:234 (extended abstract)
2. Rice DB (1993) Power 6:103
3. Sullivan P, Hepburn BJ (1993) Industrial Water Treat 11/12:52
4. Neagle W (1994) Surface and interface characterization in corrosion. NACE International, Houston, Texas
5. Puckorius PR, Strauss SD (1995) Power 5:17
6. Sullivan PJ, Young T, Garey J (1996) Industrial Water Treat 11/12:39
7. Kármán FH, Felhôsi I, Kálmán E, Cserny I, Kôvér L (1998) Electrochim Acta 43:69
8. Gusmano G, Montesperelli G, Traversa E (1992) Mat Sci Forum 111/112:313
9. Felhôsi I, Keresztes Zs, Kármán FH, Mahai M, Bertóti I, Kálmán E (1999) J Electrochem Soc 146:961
10. Ramesh S, Rajeswari S (2004) Electrochim Acta 49:811
11. Gabrielli C, Keddam M, Maurin G, Perrot H, Rosset R, Zidoune M (1996) J Electroanal Chem 412:189
12. Neville A, Morizot AP, Hodgkiess T (1998) Mater Perform 5:50
13. Deslouis C, Festy D, Gil O, Rius G, Touzain S, Tribollet B (1998) Electrochim Acta 43:1891
14. Khalil A, Rosset R, Gabrielli C, Keddam M, Perrot H (1999) J Appl Electrochem 29:339
15. Morizot A, Neville A, Hodgkiess T (1999) J Cryst Growth 198/199:738
16. Neville A, Hodgkiess T, Morizot AP (1999) J Appl Electrochem 29:455

17. Jaouhari R, Benbachir A, Guenbour A, Gabrielli C, García-Jareno J, Maurin G (2000) J Electrochem Soc 147:2151
18. Barchiche Ch, Deslouis C, Festy D, Gil O, Refait Ph, Touzain S, Tribollet B (2003) Electrochim Acta 48:1645
19. Marín-Cruz J, González I (2002) J Electrochem Soc 149:B1
20. Marín-Cruz J, García-Figueroa E, Miranda-Hernández M, González I (2004) Water Res 38:173
21. Marín-Cruz J, Cabrera-Sierra R, Pech-Canul M, González I (2004) J Appl Electrochem 34:337
22. Hartt WH, Culberson CH, Smith WS (1984) Corrosion 40:609
23. Libutti BL, Knudsen JG, Muller RW (1984) Mater Perform 11:47
24. Lin SH, Dexter SC (1988) Corrosion 44:615
25. Gabrielli C, Keddam M, Khalil A, Maurin G, Perrot H, Rosset R, Zidoune M (1998) J Electrochem Soc 145:2386
26. Gabrielli C, Maurin G, Poindessous G, Rosset R (1999) J Cryst Growth 200:236
27. Marín-Cruz J, Cabrera-Sierra R, Pech-Canul MA, González I (2006) Electrochim Acta 51:1847
28. Kuznetsov Yurii I (2004) Russ Chem Rev 73:75
29. Boffardi BP (1999) ASHRAE J 41:52